Journal of Quantitative Spectroscopy & Radiative Transfer 110 (2009) 1147–1161

Contents lists available at ScienceDirect

Journal of Quantitative Spectroscopy & Radiative Transfer

journal homepage: www.elsevier.com/locate/jqsrt

# Impact of the non-measured infrared spectral range of the imaginary refractive index on the derivation of the real refractive index using the Kramers–Kronig transform

M. Segal-Rosenheimer *, R. Linker

*Faculty of Civil and Environmental Engineering, Technion – Israel Institute of Technology, Haifa 32000, Israel*

ARTICLE INFO

*Article history:*
Received 15 February 2009
Received in revised form
18 March 2009
Accepted 19 March 2009

*Keywords:*
Kramers–Kronig
Mid-IR
Ammonium sulfate
Water droplets
Optical constants

ABSTRACT

A quantitative analysis to asses the influence of a non-measured imaginary index spectrum on the extracted real refractive index is presented. The investigation was done on the Mid-IR spectral range, where the "measured" imaginary spectrum is defined between 800 and 4500 $cm^{-1}$. The influence of bands of various locations and shapes in the non-measured IR spectral region (0–800 $cm^{-1}$) on the $n$ values obtained by the computational procedure of the Kramers–Kronig transform was investigated. Additional analysis was conducted to estimate the relevance of different assumptions that are commonly made with regard to the non-measured range (e.g. linear extrapolation or the effect of uncertainty in the precise band location). The results show that the contribution of an unmeasured band at any wavenumber $\tilde{\nu}_0$ is well described by a simple function of the band location and $\tilde{\nu}_0$, regardless of the band shape. Furthermore, the error caused by incorrect band location can also be described by a simple function of the band location, the band location error and $\tilde{\nu}_0$. The simple functions can be used to estimate the impact that ignoring or misplacing a band will have on the extracted $n$ spectrum, without performing the whole KK integration. These relationships were validated on two data sets of optical constants of crystalline ammonium sulfate and water in the Mid-IR range.



## 1. Introduction

Quantitative analysis of remote sensing and laboratory broadband spectroscopic measurements of aerosols relies on the accurate knowledge of their complex refractive index ($N(\tilde{\nu}) = n(\tilde{\nu}) + ik(\tilde{\nu})$) in the spectral region of interest. The imaginary part ($k(\tilde{\nu})$) is usually estimated using spectra of a thin film of the investigated material or transmission spectra of small particles. The real part ($n(\tilde{\nu})$) can then by derived for instance using the Kramers–Kronig transform (KKT) [1] that relates $n$ and $k$ according to

$$n(\tilde{\nu}_0) - 1 = \frac{2}{\pi} P \int_0^{\infty} \frac{k(\tilde{\nu})\tilde{\nu}}{\tilde{\nu}^2 - \tilde{\nu}_0^2} d\tilde{\nu} \tag{1}$$

where $n(\tilde{\nu}_0)$ denotes the real part of the refractive index at the wavenumber of interest, $\tilde{\nu}_0$, $k(\tilde{\nu})$ denotes the imaginary part of the refractive index at the wavenumber $\tilde{\nu}$, and $P$ means the Cauchy principal part of the integral should be taken.

* Corresponding author. Tel.: +972 4 8292808; fax: +972 4 8228898.
*E-mail addresses:* segalm@tx.technion.ac.il (M. Segal-Rosenheimer), linkerr@tx.technion.ac.il (R. Linker).

0022-4073/$ - see front matter © 2009 Elsevier Ltd. All rights reserved.
doi:10.1016/j.jqsrt.2009.03.017

This powerful mathematical relation is frequently used in the extraction procedures of optical constants in the mid-IR spectral region [2–8] since it allows extraction of the whole $n$ spectrum from any "given" $k$ spectrum. Its strength lies in the fact that it ties both indices into one mathematical relation, allowing straightforward calculation of $n$ from a single spectral measurement. This is especially important in the mid-IR spectral range, where the $k$ component exhibits a great variability and high intensities, which cannot be neglected as sometimes done in the visible range [1]. However, it is clear from Eq. (1) that this integration procedure requires the knowledge of $k$ over the whole spectral range—from zero to infinity. In practice, of course, this demand cannot be satisfied, as the transmission or absorption measurements are made over a finite spectral range. Therefore, when performing the KKT calculation on a measured $k$ spectrum, one needs to assume its behavior beyond the measured spectral range.

Several investigations [5,8–10] have emphasized the need to extrapolate the truncated experimental spectrum to lower wavenumbers in order to obtain a better estimate of $n$ via the KKT procedure. Myhre et al. [10] have shown with a synthetic water spectrum and data of aqueous sulfuric acid that truncation of the $n$ spectrum below 500 $cm^{-1}$ affects the final refractive index values extracted by the KKT procedure (corresponding to reflectance and not transmission measurements). They concluded that neglecting the lower wavenumber range in the KKT procedure will cause an overestimation of the $n$ spectrum. Also, Wagner et al. [8], in their investigation on supercooled water droplets have shown differences in $n$ values calculated by the KKT using two different integration ranges (400–6000 and 70–6000 $cm^{-1}$). Similarly to Myhre et al. [10], Wagner et al. [8] reported that integration over the wider spectral range gave smaller values. The above investigations were done for a specific compound, and the influence of the integration range on $n$ was not investigated in a systematic fashion. Hawranek and Jones [11] have made the most significant contribution on this issue. In their study, they analyzed how truncating a band wing or neglecting a band that is located out of the measurement range causes an error in $n$ calculated using either the KKT or the subtractive-KKT procedure. However, their work was related only to a very narrow spectral band and although their conclusions include very pertinent observations, these cannot be used directly to estimate in a straightforward fashion the error caused by common assumptions (for instance linear extrapolation of the spectrum or neglecting a band at an arbitrary location). Since the KKT procedure is a common method for the extraction of optical constants, a general approach to asses the influence of the absorption features in the spectral range beyond the measurement limits would be useful. Such a tool would provide a quantitative criterion for deciding whether extrapolation of the $k$ spectrum beyond the actual measurement's range is desirable and what type of extrapolation would be most appropriate.

In addition, in remote sensing applications, a tool that provides an estimation of the confidence interval for the optical constants so that the error in the extinction calculations can be obtained might be useful. For example, instruments such as ATMOS (Atmospheric Trace Molecular Spectroscopy) and FTS (Fourier Transform Spectrometer) that cover spectral ranges of 800–5200 and 750–4100 $cm^{-1}$, respectively, [12] need only optical constants in the respective measurement range to derive aerosol characteristics. However, this is somewhat misleading since the optical constants used in such applications were not necessarily derived from the whole spectral range, meaning that their derivation may have neglected important, unmeasured bands. Clearly, such inaccuracy of the optical constants will affect the accuracy of retrieved aerosol characteristics. Hence, a quantitative approach that enables the assessment of a confidence interval for the optical constants will allow better assessment of the validity of the results obtained from such measurements.

In the present study, we investigated the influence of bands of various locations and widths in the non-measured spectral region on the $n$ values calculated by the KKT procedure. The non-measured spectral region refers to the low wavenumber interval (below 800 $cm^{-1}$) that is not covered by most common mid-IR detectors. The net contribution of the non-measured spectral range was estimated under various assumptions (i.e. different band locations, widths and shapes). An additional analysis was conducted to assess the relevance of several assumptions that are commonly made when applying the KKT procedure. The results were implemented on two data sets of optical constants of crystalline ammonium sulfate and water droplets with different size distributions to illustrate the use of the present results for real applications.

## 2. Procedure

### 2.1. General considerations

Since experimental (e.g. by remote sensing or in the laboratory) spectra are always restricted to a finite spectral range, using the KKT always requires some assumptions regarding the spectrum in the spectral range beyond the measurement limits. The experimental spectral range of interest in the current study lies in the Mid-IR, and more specifically the 800–4500 $cm^{-1}$ range. The reason for choosing this range as the "measured" spectrum was that many experimental investigations on optical constants in the IR range are restricted to this range [3,5,8,13–15]. Although in some investigations the measurement range extended down to 600 $cm^{-1}$ [16], 500 $cm^{-1}$ [2,6], or even 400 $cm^{-1}$ [10,17], such studies are quite rare due to hardware limitations (detectors and optics).

In order to analyze the influence of the truncation on the KKT calculation, the integral's infinite integration range was divided into four distinct spectral regions (i.e. Far-IR, Mid-IR, visible and UV) following Biermann et al. [2]:

$$n(\tilde{\nu}_0)-1=\frac{2}{\pi}\left\{\underbrace{P\int_0^{800}\frac{k(\tilde{\nu})\tilde{\nu}}{\tilde{\nu}^2-\tilde{\nu}_0^2}d\tilde{\nu}}_{\text{Non-measured IR range}}+\underbrace{P\int_{800}^{4500}\frac{k(\tilde{\nu})\tilde{\nu}}{\tilde{\nu}^2-\tilde{\nu}_0^2}d\tilde{\nu}}_{\text{Measured IR range}}+\underbrace{P\int_{4500}^{50{,}000}\frac{k(\tilde{\nu})\tilde{\nu}}{\tilde{\nu}^2-\tilde{\nu}_0^2}d\tilde{\nu}}_{\text{Non-measured VIS range}}+\underbrace{P\int_{50{,}000}^{\infty}\frac{k(\tilde{\nu})\tilde{\nu}}{\tilde{\nu}^2-\tilde{\nu}_0^2}d\tilde{\nu}}_{\text{Non-measured UV range}}\right\} \tag{2}$$

As most of atmospheric components do not have absorption features in the visible spectral range, its influence on the final KKT procedure can be neglected [2]. Furthermore, as in the integral over the UV region the wavenumber $\tilde{\nu}$ is much larger than $\tilde{\nu}_0$, this term is almost independent of $\tilde{\nu}_0$ and can be approximated as a constant [2]. In the literature, the sum of this positive constant and the constant "1" that appears in the left side of the KKT equation (shown in Eqs. (1) and (2)), is usually denoted as $n(\infty)$. Following these considerations, the present study focused on the influence of the non-measured IR range (0–800 $cm^{-1}$) when using the KKT procedure to derive $n$. The goal was to estimate the error introduced to the estimated $n$ values by various assumptions about the $k$ spectrum. The most commonly used assumptions are: (1) neglecting the non-measured $k$ spectrum altogether ("spectrum truncation"), (2) extrapolating (most often linearly) the measured spectrum from the last measured value down to zero at 0 $cm^{-1}$, and (3) appending to the measured spectrum band(s) based on literature. This study investigated in a systematic fashion the influence of each of these assumptions on the $n$ spectrum calculated using the KKT procedure. Although the subtractive KKT procedure is also widely used and is considered as a more accurate under spectral uncertainties (e.g. [8,11]), extension of the present analysis to the subtractive KKT procedure, which assumes the knowledge on an anchor value of $n$ within the measurement range, is beyond the scope of this study.

### 2.2. Spectrum truncation

The first set of calculations was performed to determine the error caused by neglecting the 0–800 $cm^{-1}$ range altogether. Clearly, according to Eq. (2) this results in consistent overestimation of $n$. It must be noted that the neglected term is independent of the measured spectrum $k$, and in the sequel is termed the *absolute truncation error*. This error was evaluated by constructing synthetic spectra with bands of various shapes at various locations within the 0–800 $cm^{-1}$ range and calculating the corresponding integral of the KKT procedure. Two types of band shapes were tested: Gaussian and Lorentzian. Eq. (3) shows a $k$ spectrum that consists of a single Gaussian band located at $\mu$ $cm^{-1}$ and which has a standard deviation of $\sigma$ $cm^{-1}$.

$$k(\tilde{\nu})=G(\tilde{\nu})=\frac{1}{\sqrt{2\pi}\sigma}\exp^{-(\tilde{\nu}-\mu)^2/2\sigma^2} \tag{3}$$

Ninety-nine percent of the band lies within the $\mu\pm3\sigma$ interval and in the sequel we refer to $6\sigma$ as the "bandwidth". Note that the band area was normalized to unity since one of the objectives was to determine the influence of the band shape (and not amplitude) on the truncation error. Clearly, according to Eq. (2), changing the band amplitude while keeping its shape ($\mu$ and $\sigma$) unchanged acts as a simple scaling factor. Spectra were generated with band center ranging from 90 to 710 $cm^{-1}$ at 4 $cm^{-1}$ increments and standard deviation values ranging from 1 to 26 $cm^{-1}$ (at 1 $cm^{-1}$ increment). The contribution of this band (first right-hand side term in Eq. (2)) was evaluated at each $\tilde{\nu}_0$ within the measurement range (i.e. 800–4500 $cm^{-1}$).

Spectra with Lorentzian bands were generated in a similar manner:

$$k(\tilde{\nu})=L(\tilde{\nu})=\frac{1}{2\pi}\frac{\Gamma}{(\tilde{\nu}-\mu)^2+(\Gamma/2)^2} \tag{4}$$

where $\Gamma$ is the width at half maximum, which was also varied from 1 to 26 $cm^{-1}$ at 1 $cm^{-1}$ increments.

### 2.3. Linear extrapolation

Linear extrapolation of the measured spectrum is commonly used as a correction factor when applying the KKT procedure [2]. Therefore, the contribution of such a correction term was estimated in a systematic fashion for various slopes. Since the spectrum is extrapolated to zero (at 0 $cm^{-1}$), this slope is directly dictated by the absorbance measured at the lowest wavenumber. In most cases those values are relatively low [3,5,6], and hence in the present study $k$ values between 0 and 0.12 were considered.

### 2.4. Literature-based extrapolation

A better way to take into account the non-measured range of the $k$ spectrum is to append to the measured spectrum values from the literature or from an electronic database. However, such databases are not always readily available in a high resolution digitized form, so that the location of specific bands cannot always be estimated accurately. Also, as the "literature" spectrum was recorded under different experimental conditions, a scaling adjustment should be made. Nevertheless, this method is believed to be more accurate, as shown in several investigations [3,5,14,18].

In the present study, we investigated in a systematic fashion the residual error in $n$ that is caused by imperfect literature-based $k$ spectrum extrapolation. More specifically, we calculated the error caused at every $\tilde{\nu}_0$ by: (1) incorrect location of the appended band and (2) incorrect shape of this band. This was done by comparing the KKT contribution of a "true" band (chosen values for the band center, $\mu$, and shape, $\sigma$ or $\Gamma$) with the contribution obtained after modifying slightly the band location and/or shape. This comparison was performed at every $\tilde{\nu}_0$ and the calculations were repeated with various values of the band shift (denoted $\Delta\mu$) and the band shape (denoted $\Delta\sigma$ or $\Delta\Gamma$), so that it was possible to derive an analytical expression for the residual error in $n$ at any $\tilde{\nu}_0$.

## 3. Results and discussion

### 3.1. Spectrum truncation

Fig. 1 shows the error that results from truncating the spectrum and ignoring a single (unmeasured) Gaussian band centered at $\mu\,\mathrm{cm}^{-1}$ with standard deviation $\sigma$ equal to 2 and 26 $\mathrm{cm}^{-1}$ (top and bottom frames, respectively). Although in practice the neglected spectral interval may contain multiple bands, it is clear from the linearity of Eq. (2) with respect to $k$ that the contributions of these bands will simply add-up so that considering a single band does not reduce the generality of these results. As expected from Eq. (2), the $n$ spectrum is always overestimated in the range of the $k$ measurement (800–4500 $\mathrm{cm}^{-1}$) and the largest errors occur when the location of the neglected band is close to $\tilde{\nu}_0\,\mathrm{cm}^{-1}$. This result is

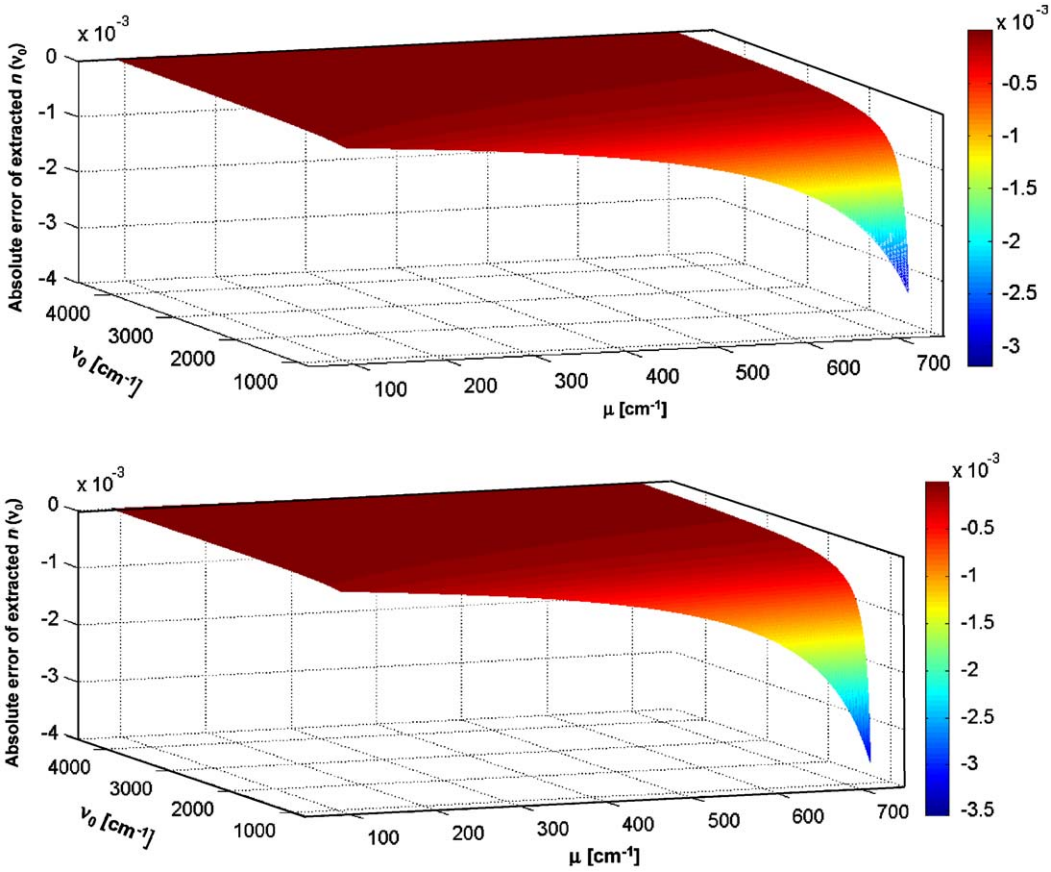


**Fig. 1.** Absolute error "added" to the extracted $n$ value in the 800–4500 $\mathrm{cm}^{-1}$ range ($\nu_0$) as a function of the location ($\mu$) of a unmeasured Gaussian band with a bandwidth of 12 $\mathrm{cm}^{-1}$ (top frame) and 156 $\mathrm{cm}^{-1}$ (bottom frame), which correspond to standard deviation values ($\sigma$) of 2 and 26, respectively.

consistent with Myhre et al. [10] that found that the estimated index of refraction decreases when the integration range is increased. Wagner et al. [8] in their analysis on optical constants of water droplets have also shown that the real part of the refractive index decreases when the KK integration is performed on a wider spectral range (given, of course that an absorption band exists in the lower frequency range). Fig. 1 shows that the effect is close to exponential, so that neglecting a band centered around 700 $cm^{-1}$ causes a large overestimation of $n$ at the wavenumbers close to the spectrum cutoff (800 $cm^{-1}$). Similar trends were also shown by Hawranek and Jones [11]. The error is reduced by 70% at 1000 $cm^{-1}$, and by over 80% at wavenumbers above 1500 $cm^{-1}$. At about 2500 $cm^{-1}$, the error due to neglecting an absorbance band below 800 $cm^{-1}$ is only 2% of the error at 800 $cm^{-1}$.

According to Eqs. (2) and (3), the error does not only depend on the band location but depends also on the band shape, represented here by $\sigma$. As $\sigma$ increases, the error in $n$ increases. However, comparison between the top and bottom frames of Fig. 1 shows that for the range of realistic values investigated ($1 \leqslant \sigma \leqslant 26$) the band shape influences the error only marginally. The largest deviation, which amounts to 12% of the error, is obtained when the neglected band is close to the measurement region (i.e. high $\mu$ and low $\nu_0$). By comparison, a difference of 50 $cm^{-1}$ in band location yields a maximal difference of almost 40%, for the same band shape and at low $\nu_0$, which shows that the KKT procedure is much more sensitive to band location than to band shape.

Although the absolute values in Fig. 1 might seem very small, it must be noted that the above calculations were done using normalized bands with unit area. Hence, the actual band "size" must be taken into account when deciding whether the absolute error is negligible or not (see Section 3.4).

A similar analysis with Lorentzian bands yielded very similar results, and in particular larger $\Gamma$ values, which correspond to wider bands, gave slightly higher absolute error values (details not shown).

Since the neglected integral depends on $(\tilde{\nu}^2 - \tilde{\nu}_0^2)$ (Eq. (2)), it does not strictly depend on the distance between the location of the neglected band ($\mu$) and the location $\tilde{\nu}_0$ were the $n$ spectrum is estimated. Indeed, Fig. 2, which shows the error in the extracted $n$ spectrum as a function of this distance, shows that the error depends not only on $(\mu - \tilde{\nu}_0)$ but also on $\mu$ itself. However, the dependence on $\mu$ is quite small, so that the error caused by a neglected band can be estimated quite well based only on its distance from the wavenumber $\tilde{\nu}_0$ of interest. In other words, the estimation error of $n$ at 900 $cm^{-1}$ caused by neglecting a band located at 500 $cm^{-1}$ is almost equal to the estimation error of $n$ at 1100 $cm^{-1}$ that would be caused by neglecting a band located at 700 $cm^{-1}$. Mathematically, the relationship between the estimation error $\Delta n(\tilde{\nu}_0)$ and $(\mu - \tilde{\nu}_0)$ is well described ($R^2 = 0.97$) by the following function:

$$\Delta n(\tilde{\nu}_0) = \frac{\alpha}{(\tilde{\nu}_0 - \mu)^{\beta}} \tag{5}$$

where $\Delta n(\tilde{\nu}_0)$ is the $n$ contribution of the non-measured range with $\alpha = -2.33$ and $\beta = 1.4$ regardless of the band type (Gaussian or Lorentzian). Alternatively, it is possible to obtain a more accurate relationship for any given $\mu$, which yields the coefficients $\alpha(\mu)$ and $\beta(\mu)$ shown in Fig. 3. As indicated on the figure, $\alpha(\mu)$ and $\beta(\mu)$ can be described by an exponential and linear function of $\mu$, respectively, so that Eq. (5) can be rewritten as

$$\Delta n(\tilde{\nu}_0) = \frac{48.01\ \exp(-17.3 \times 10^{-3}\mu) - 50.93\ \exp(-5.78 \times 10^{-3}\mu)}{(\tilde{\nu}_0 - \mu)^{(1.95 - 1.06 \times 10^{-3}\mu)}} \tag{6}$$

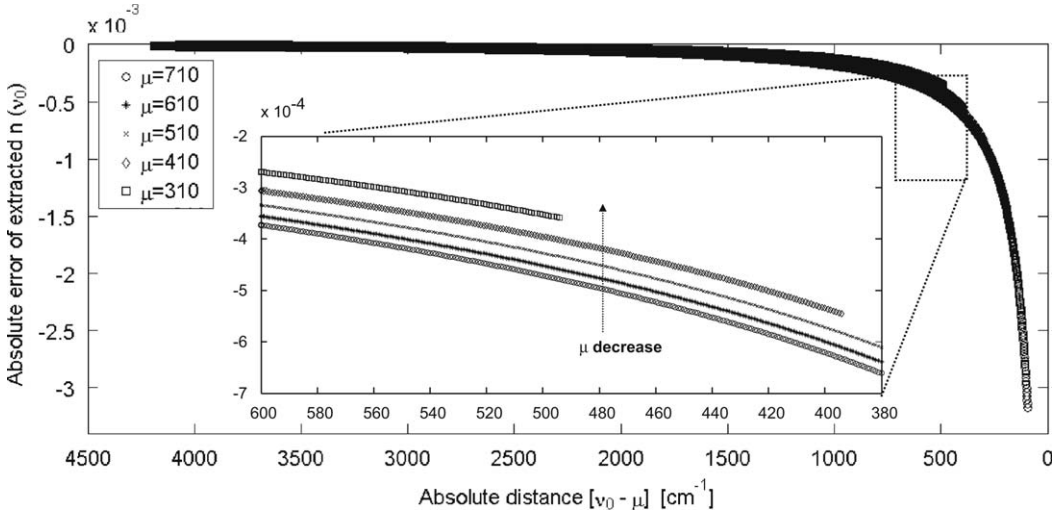


**Fig. 2.** Absolute error "added" to the calculated $n$ value as a function of the absolute distance of the wavenumber of interest ($\nu_0$) and the location of the neglected band ($\mu$). Values are shown for Gaussian bands with standard deviation of 2 $cm^{-1}$.

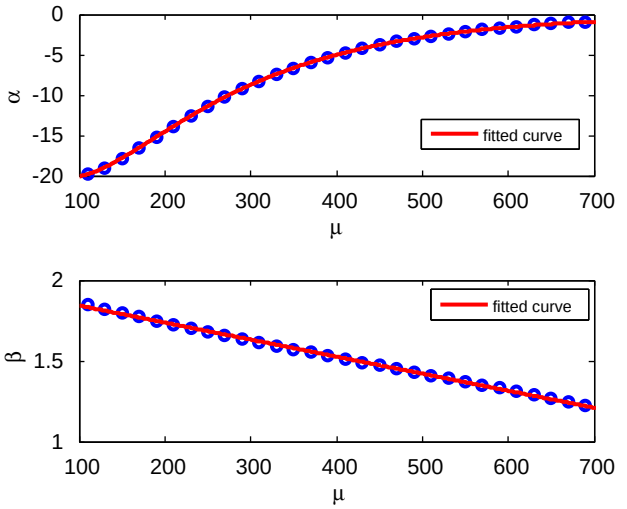


**Fig. 3.** Coefficients $\alpha$ (top frame) and $\beta$ (bottom frame) introduced in Eq. (5), as a function of the band location, $\mu$. Fitted functions, exponential (top frame) and linear (bottom frame), respectively, are also shown.

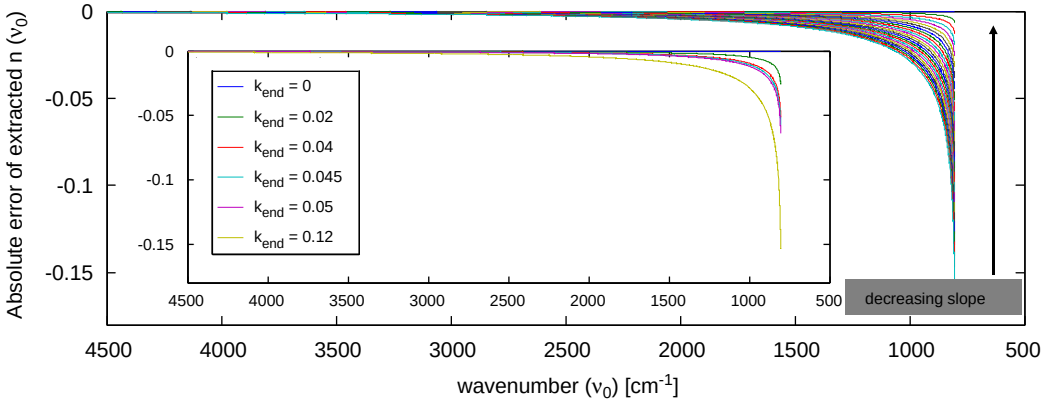


**Fig. 4.** Absolute $n$ error values as a function of different line slopes based on a linear extrapolation of the measured spectrum. The range of $k_{end}$ is the same in both panels and only selected values are presented in the inner panel for clarity. (For interpretation of the references to colour in this figure legend, the reader is referred to the web version of this article.)

Eq. (5) was obtained assuming that the whole band lies in the 0–800 $cm^{-1}$ range and has no tail beyond 800 $cm^{-1}$. In practice, if the band is very broad and/or close to 800 $cm^{-1}$, a significant portion of the band may indeed lie beyond 800 $cm^{-1}$. In such cases, Eqs. (5) and (6) would overestimate the contribution of this band and a correction factor needs to be included. Eq. (5) is therefore rewritten as

$$\Delta n(\tilde{\nu}_0) = \frac{\alpha}{(\nu_0 - \mu)^{\beta}} P\{G(\mu,\sigma) < 800\} \tag{7}$$

for the Gaussian case, and

$$\Delta n(\tilde{\nu}_0) = \frac{\alpha}{(\nu_0 - \mu)^{\beta}} P\{L(\mu,\Gamma) < 800\} \tag{8}$$

for the Lorentzian case. In both expressions, $P$ denotes the cumulative probability of the respective function to be below 800.

Using either expression, it is possible to estimate the error caused in the 800–4500 $cm^{-1}$ range by neglecting any band located within the 90–710 $cm^{-1}$ interval investigated in this study. The calculation is straightforward and does not require KK integration, and the only information required from the user is the location of the neglected band.

### 3.2. Linear extrapolation

Fig. 4 shows the absolute $n$ error at each $\tilde{\nu}_0$, for various slopes of the appended "spectrum". As expected, linear extrapolation of the measured spectrum affects primarily the $n$ estimation at wavenumbers close to the spectral cutoff. Also, the larger the slope, the larger the absolute $n$ error. It may be noted that the absolute $n$ error values are much larger than the values calculated in the previous section for the normalized absorption bands. However, it must be remembered that in practice the unmeasured bands must be scaled according to their expected (guessed) intensity, so that linear extrapolation can lead either to over- or under-estimation of the final $n$ as will be shown below (Section 3.4). The results shown in Fig. 4 were fitted by a double exponential function ($\alpha \exp(\beta\tilde{\nu}_0) + \gamma \exp(\eta\tilde{\nu}_0)$) that describes well ($R^2 = 0.98$) the "added" $n$ values at each $\tilde{\nu}_0$. The coefficients $\alpha$ and $\gamma$ depend linearly on the last value of the measured $k$ spectrum, $k_{end}$, as shown in

$$\Delta n(\tilde{\nu}_0) = (-8.14 \times 10^6 k_{end} + 77.14)\exp(-0.0201\tilde{\nu}_0) + (-1.201 k_{end} + 1.28 \times 10^{-6})\exp(-0.0018\tilde{\nu}_0) \quad (9)$$

### 3.3. Literature-based extrapolation

Intuitively, for those cases when literature data relative to the unmeasured spectral range are available, it seems natural that appending to the measured $k$ spectrum one or several artificial "literature band(s)" should yield more accurate estimate of $n$. Ideally, adding a band with the right size and shape at the correct location, would cancel the error. However, in practice neither the location nor the shape and size of the appended band are correct and the following questions arise: How sensitive is the correction procedure to: (1) mismatch between the true and estimated (literature-based) band location and (2) mismatch between the true and estimated band shape. Although mismatch between the overall intensity of the true and estimated band is also a cause of error, if the band location and shape are correct such a mismatch acts as a scaling factor on the error and hence does not require further investigation.

Fig. 5 shows a contour plot of the difference between the contribution of a true and "literature-based" band on the $n$ spectrum estimate at $\tilde{\nu}_0 = 1000\,\mathrm{cm}^{-1}$, for a true band centered at $\mu = 380\,\mathrm{cm}^{-1}$ with $\sigma = 13\,\mathrm{cm}^{-1}$ and a literature band centered at $\{\mu - \Delta\mu\}$ with width $\{\sigma - \Delta\sigma\}$. This contour plot clearly shows that assuming an incorrect band shape ($\Delta\sigma$) has virtually no influence on the error. On the contrary, the error is sensitive, in a non-symmetric way, to assuming an incorrect band location. For instance, locating the "appended" band $100\,\mathrm{cm}^{-1}$ beyond or below its true location yields a residual error of $0.12 \times 10^{-3}$ and $-0.08 \times 10^{-3}$, respectively. For comparison, according to Fig. 2 (or Eq. (5)), neglecting this band altogether would yield an error equal to $0.275 \times 10^{-3}$. This clearly shows that if a reasonable estimate of the location (and overall intensity) of an unmeasured band is available, adding this band is preferable over neglecting it altogether (as long as the localization error is $<\sim 200\,\mathrm{cm}^{-1}$ in the present case). Fig. 5 also shows that the error caused by placing a band at lower wavenumbers than its true location is smaller than if the band is shifted by the same amount to higher wavenumbers.

This analysis was repeated with a Lorentzian-shaped band and similar trends were observed (details not shown). In particular, the $\Gamma$ parameter did not affect much the calculated $n$, and the same asymmetry of $\Delta n$ was observed.

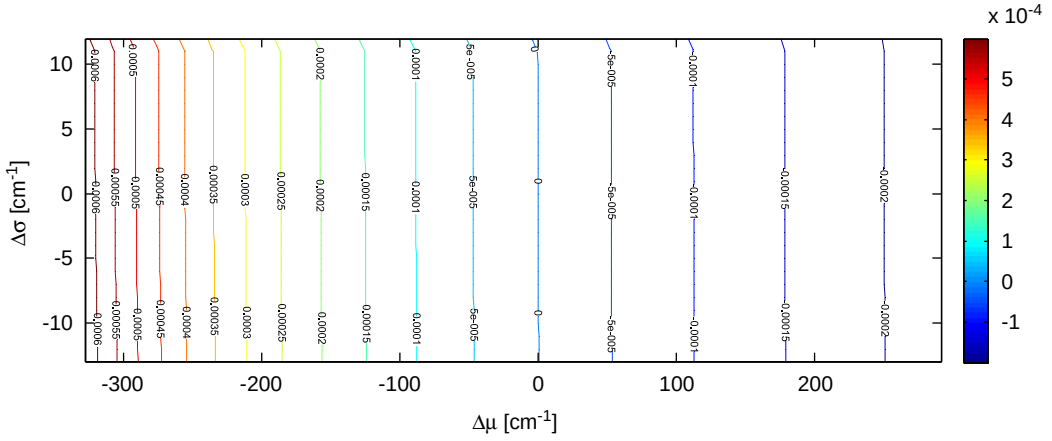


**Fig. 5.** Residual $n$ error values, at $\nu_0 = 1000\,\mathrm{cm}^{-1}$, calculated based on the assumption that the true band is located at $380\,\mathrm{cm}^{-1}$ with a Gaussian standard deviation ($\sigma$) of $13\,\mathrm{cm}^{-1}$, while the added band is located at $\{\mu-\Delta\mu\}$ with width $\{\sigma-\Delta\sigma\}$ as detailed in the text.

While the results presented in Fig. 5 correspond to a specific $\mu$ and $\tilde{\nu}_0$, by performing similar calculations with various $\mu$ and $\tilde{\nu}_0$ and neglecting the influence of the shape mismatch ($\Delta\sigma$), it was possible to find a relationship between the relative residual error at any $\tilde{\nu}_0$ ($\Delta n(\tilde{\nu}_0)/n^*(\tilde{\nu}_0)$), the true band location ($\mu$) and the band location mismatch ($\Delta\mu$):

$$\frac{\Delta n(\tilde{\nu}_0)}{n^*(\tilde{\nu}_0)} = \phi\Delta\mu \tag{10}$$

where $n^*(\tilde{\nu}_0)$ is the contribution of the Gaussian located at its correct location (*absolute truncation error*) and $\Delta n(\tilde{\nu}_0)$ is the residual error due to the location mismatch ($\Delta\mu$). The parameter $\phi$ is not constant but depends on $\tilde{\nu}_0$, $\mu$ and the sign of $\Delta\mu$ (Figs. 6 and 7). Fig. 7 shows that $\phi$ can be approximated as follows ($R^2 > 0.99$):

$$\phi = \frac{1}{\mu} + a\left[\frac{1}{4500^b} - \frac{1}{(\mu - \tilde{\nu}_0)^b}\right] \tag{11}$$

with

$$a = 5.789 \quad \text{and} \quad b = 1.298 \ \text{ for } \Delta\mu < 0$$

$$a = -1.435 \quad \text{and} \quad b = 1.887 \text{ for } \Delta\mu > 0$$

By using Eqs. (10) and (11) together with Eq. (6), it is possible to estimate in a straightforward manner upper bounds on the error (confidence interval) that will be introduced at any location of the 800–4500 $\text{cm}^{-1}$ $n$ spectrum by a "corrective" Gaussian band that is not perfectly well located. While in principle the same confidence interval could be obtained by repeating calculations with Eq. (6) with different values of $\mu$, Eqs. (10)–(11) make it possible to estimate the confidence interval in a simpler and direct fashion.

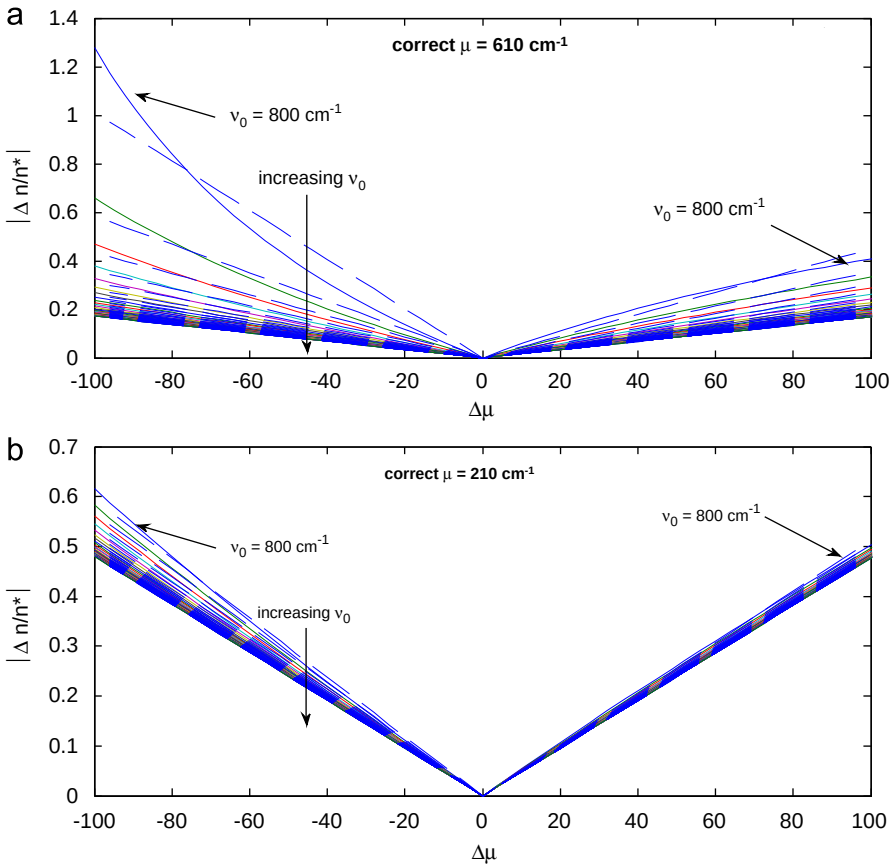


**Fig. 6.** Relative error values obtained by dividing the error due to a mismatch in the $\mu$ location ($\Delta n$, as shown in Fig. 5 contour lines) by the absolute error caused by neglecting a band at its correct location ($n^*$ in figure). The "real" relative error values (solid lines) were fitted using Eq. (10) (blue dashed lines). Each line was calculated for a separate $\nu_0$ (range between 800 and 4500 $\text{cm}^{-1}$). Frame (a) shows the calculations for a band located at $\mu = 610\,\text{cm}^{-1}$ and frame (b) for a band located at $\mu = 210\,\text{cm}^{-1}$. Note that $\Delta n/n^*$ is negative for $\Delta\mu > 0$ but for clarity absolute values are shown in the figure.

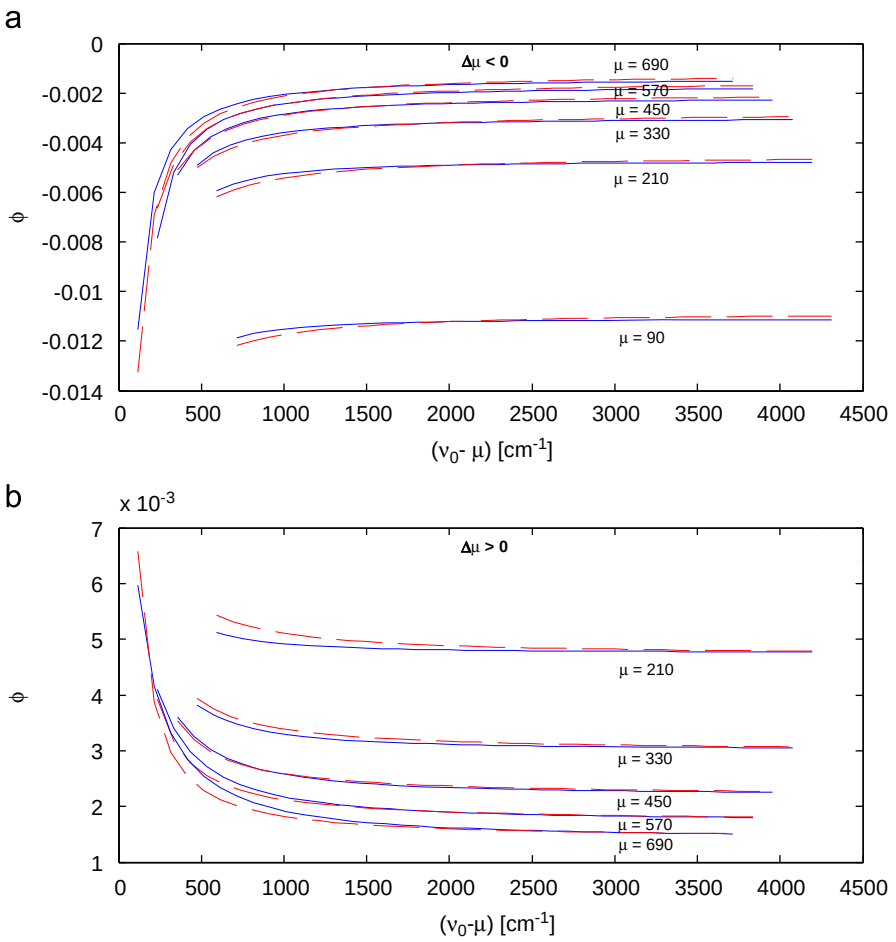


**Fig. 7.** Coefficient $\phi$ introduced in Eq. (10), for various values of $(\nu_0-\mu)$, $\mu$ and $\Delta\mu$ (red dashed line). The top and bottom frames correspond to $\Delta\mu<0$ and $\Delta\mu>0$, respectively. For each case, the fitted model (Eq. (11)) is also shown (solid blue line).

### 3.4. Case studies-atmospheric implementation

Eqs. (5)–(11) allow one to estimate the impact a given assumption with regard to the unmeasured $k$ spectrum will have on the extracted $n$ values. In order to validate these relations and illustrate their practical use, the results obtained using these relations were compared to the results of full KKT calculations of the optical constants of ammonium sulfate and water.

#### 3.4.1. Ammonium sulfate

The high resolution set of optical constants for ammonium sulfate in the 590–5000 $cm^{-1}$ range that was made available recently by Earle et al. [6] was used as a first case study. This spectrum includes a band at 614 $cm^{-1}$ that would typically not be measured. Hence, for the sake of the discussion, the $k$ values in the 800–4500 $cm^{-1}$ range were extracted to form the "measured spectrum". Fig. 8 shows the original $k$ spectrum of Earle et al. [6], together with the truncated spectrum to which Gaussian and Lorentzian band have been added. It can be seen that the Gaussian band describes the true 614 $cm^{-1}$ band much more accurately than the Lorentzian one.

In order to validate Eqs. (6)–(11), both these equations and the full KKT procedure were used to calculate $n$ after: (1) adding a Gaussian band at 614 $cm^{-1}$ (the exact location of the "unmeasured" absorption band), and (2) extrapolating the $k$ spectrum linearly beyond 800 $cm^{-1}$.

Fig. 9a shows the relative error in the $n$ values extracted by: (1) applying the full KKT procedure to the "measured" (truncated) $k$ spectrum, (2) applying the full KKT procedure to the extended $k$ spectrum ("measured" spectrum with added Gaussian), and (3) applying the KKT procedure only to the "measured" spectrum (i.e. 800–4500 $cm^{-1}$) and adding the corrective term estimated by Eq. (6). In all cases the $n$ values of Earle et al. [6] were used as reference to calculate the

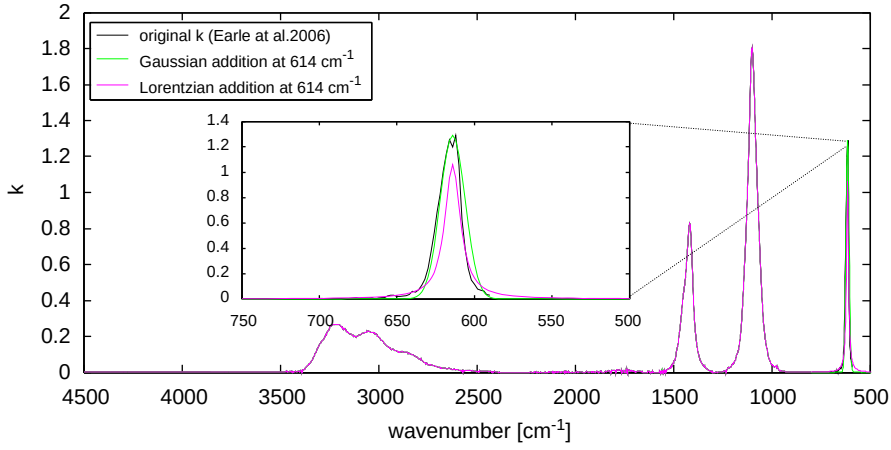


**Fig. 8.** $k$ spectra of crystalline ammonium sulfate, reproduced from Earle et al. [6] (original $k$, 4500–590 $cm^{-1}$), and extended with Gaussian or Lorentzian band additions at 614 $cm^{-1}$.

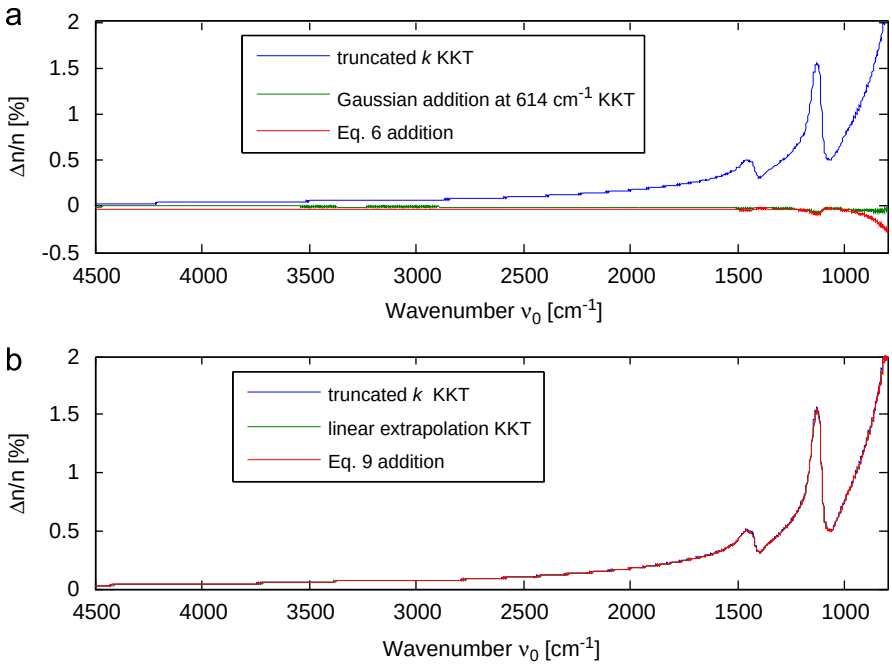


**Fig. 9.** (a) Relative $n$ error between the $n$ spectrum of Earle et al. [6] calculated by KKT over the 590–4500 $cm^{-1}$ interval and the estimates obtained with: (1) truncated 800–4500 $cm^{-1}$ $k$ spectrum, (2) addition of a Gaussian band at 614 $cm^{-1}$ to the truncated spectrum and applying the KKT procedure, and (3) truncated 800–4500 $cm^{-1}$ $k$ spectrum and the correction obtained by Eq. (6). (b) Relative $n$ error between the $n$ spectrum of Earle et al. [6] calculated by KKT over the 590–4500 $cm^{-1}$ interval and the estimates obtained with: (1) truncated 800–4500 $cm^{-1}$ $k$ spectrum, (2) linear extrapolation of the $k$ spectrum, and (3) truncated $k$ spectrum and correction obtained by Eq. (9). (For interpretation of the references to colour in this figure legend, the reader is referred to the web version of this article.)

relative error. It can be seen that very similar results are obtained using the corrective term of Eq. (6) and adding the Gaussian band and performing the KKT, which shows that the straightforward relationship obtained in Eq. (6) can indeed replace the much more complex KKT integration. It can also be seen that simply ignoring the 0–800 $cm^{-1}$ interval leads to much larger errors. In a similar way, Fig. 9b shows the relative error in the $n$ values extracted using the linear extrapolation assumption. Again, the error obtained by performing the KKT integration over the linearly extrapolated spectrum is very similar to the one obtained with the "measured" spectrum and the corrective term calculated with Eq. (9), hence validating Eq. (9). However, it must be noted that linear extrapolation of the spectrum beyond 800 $cm^{-1}$ improves the calculated $n$ only marginally, so that in the case of ammonium sulfate linear extrapolation of the $k$ spectrum is indeed a very poor correction method.

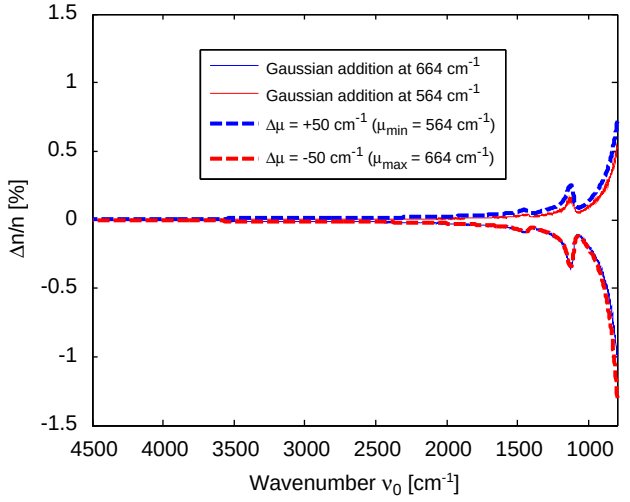


**Fig. 10.** Confidence intervals for ammonium sulfate $n$ spectrum (800–4500 $cm^{-1}$), as a result of incorrect location of the 614 $cm^{-1}$ band. The original $n$ spectrum was taken from Earle et al. [6]. Band location mismatch in the range of $\Delta\mu = \pm 50$. The confidence intervals were calculated: (1) using Eqs. (10)–(11) and (2) by applying KKT after shifting the 614 $cm^{-1}$ band artificially. (For interpretation of the references to colour in this figure legend, the reader is referred to the web version of this article.)

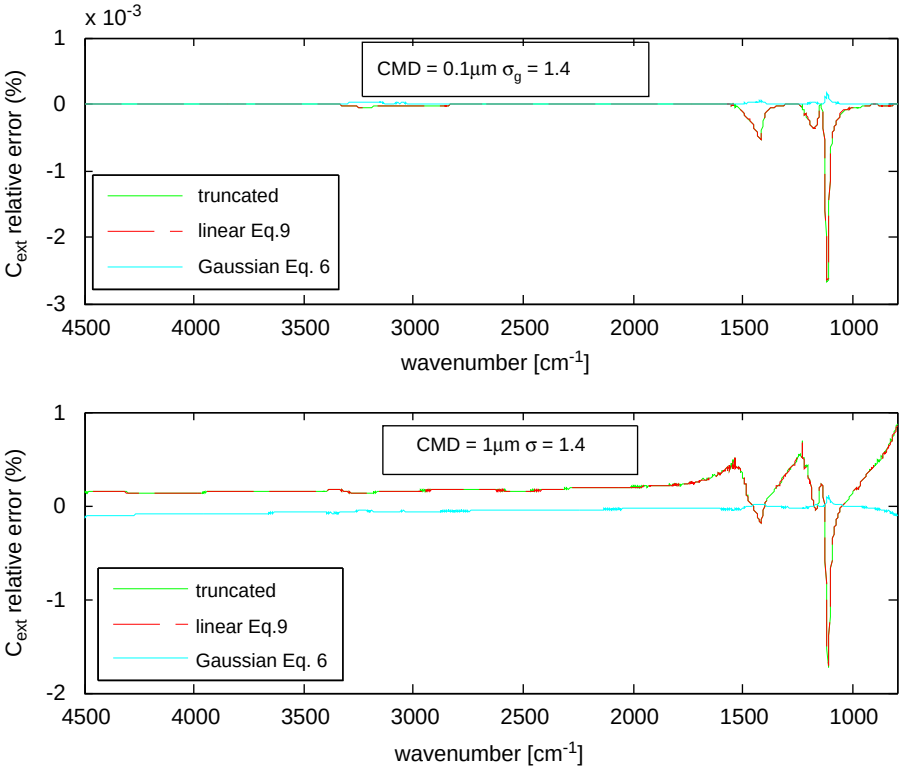


**Fig. 11.** Relative error between "real" extinction cross section calculated with the original $k$ and $n$ (Earle et al. [6]), and (1) truncated $k$, (2) truncated $k$ with correction according to Eqs. (9) and (3) truncated $k$ with correction according to Eq. (6). The calculations were made for spherical ammonium sulfate (using the Mie theory) with two different log-normal particle size distributions: (top panel) count median diameter (CMD) of 0.1 μm and a geometric standard deviation ($\sigma_g$) of 1.4, and (bottom panel) CMD of 1 μm and a $\sigma_g$ of 1.4. (For interpretation of the references to colour in this figure legend, the reader is referred to the web version of this article.)

Fig. 10 shows the relative error in $n$ that can be expected if the Gaussian band is not placed at its correct location but is shifted by up to $\pm 50\,cm^{-1}$. In order to validate Eqs. (10)–(11), the full KKT procedure was repeated after moving the Gaussian band by $\pm 50\,cm^{-1}$ (dashed lines). It can be verified that Eqs. (10)–(11) predict accurately the error caused by incorrect band location.

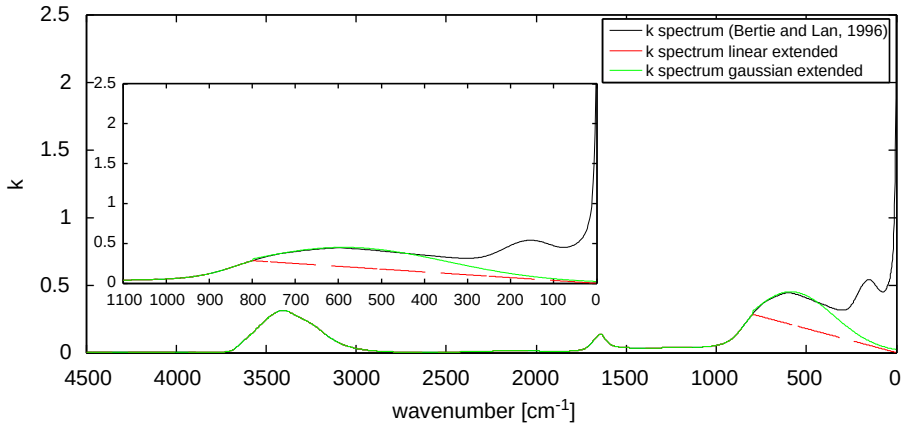


**Fig. 12.** *k* spectra of water droplets: original spectrum adopted from Bertie and Lan [9] truncated spectrum with linear and Gaussian extrapolation. (For interpretation of the references to colour in this figure legend, the reader is referred to the web version of this article.)

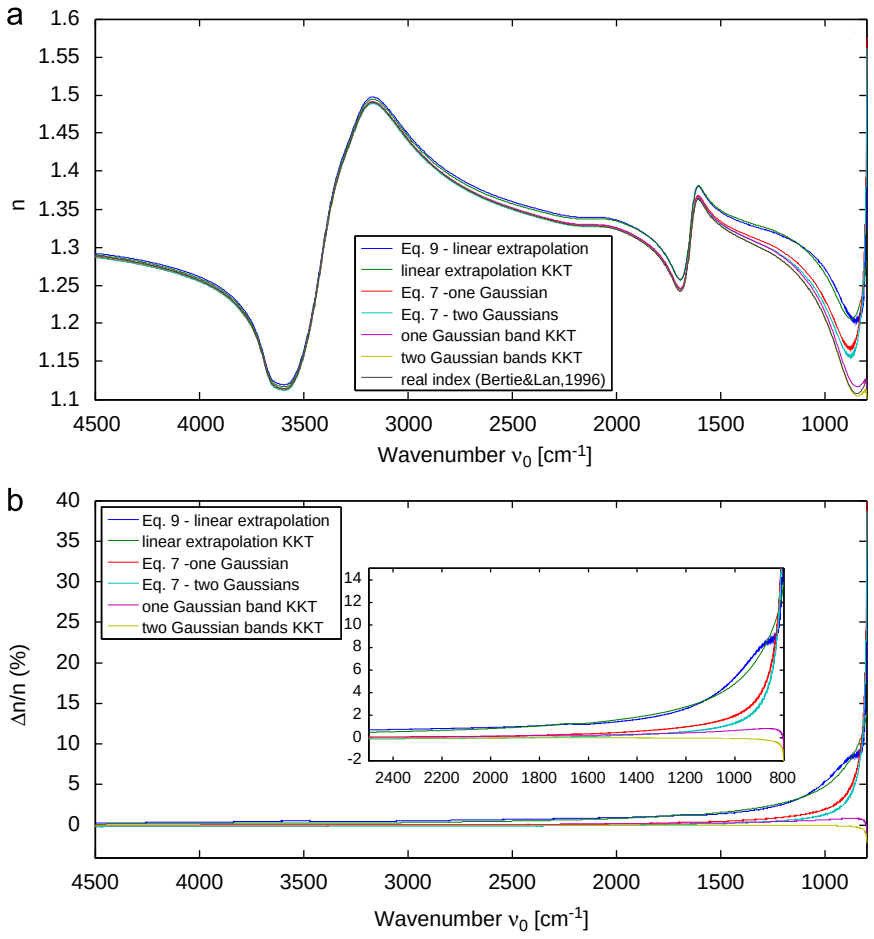


**Fig. 13.** (a) *n* spectra of water obtained by using different methods of calculation. The methods labeled "KKT" mean that *n* was obtained by applying the full KKT procedure to the extrapolated *k* spectrum. (b) Relative error of *n* (in %), for the different calculation cases introduced in (a). (For interpretation of the references to colour in this figure legend, the reader is referred to the web version of this article.)

Fig. 11 shows how the error in the *n* estimate (based on a measured *k* spectrum between 800 and 4500 $cm^{-1}$) causes an error in the estimate of the extinction cross section. Extinction calculations were done using a modification of the Bohren and Huffman [1] BHMIE code that was extended to cover the above spectral range and a log-normal size distribution. The

optical constants used for the calculation were the "measured" $k$ spectrum between 800 and 4500 $cm^{-1}$ and the $n$ spectrum: (1) obtained from the KK integral without any correction (truncated case) and (2) with correction accounting for linear extrapolation (Eq. (9)), and (3) with correction accounting for additional band at 614 $cm^{-1}$ (obtained by Eq. (6)). Errors were calculated relative to the true $k$ and $n$ of Earle et al. [6]. Although the truncated case yielded originally an error of 2.5% (Fig. 9), the final error in extinction calculations were $2.5 \times 10^{-3}$% for the small particles distribution (Fig. 11a), and up to 1.5% for the larger distribution (Fig. 11b), which shows that the influence of the optical constants inaccuracy is not constant and affects the extinction calculations only for relatively large (i.e. scattering) particles. Fig. 11 shows that the optical constants obtained using Eq. (6) yields an error close to zero, even for the largest particles. In this case, it is possible to conclude that the error due to uncertainty of the non-measured band will have only a minor effect on the final constant's values and on the extinction estimation.

### 3.4.2. Water droplets

Water is one of the most abundant component in the atmosphere, and was selected as the second case study. Fig. 12 shows the $k$ spectrum of water droplets, as assigned by Bertie and Lan [9]. As water is a molecular substance, its absorption features differ substantially compared to ammonium sulfate (ionic substance). It has two distinct regions of absorption; molecular and intermolecular. The first covers the OH molecular stretching mode at about 3300 $cm^{-1}$,and the H–O–H molecular bending mode at ~1600 $cm^{-1}$, and the second (588 $cm^{-1}$ and below) covers the intermolecular rotational and translational modes [1]. Clearly, truncation of the spectrum at 800 $cm^{-1}$ will discard many important spectral features of this substance, and as a consequence, the resulting error will be far from negligible.

Fig. 13 shows a comparison of the results of the full KKT procedure with those of the straightforward procedure based on Eqs. (6) and (9). It must be noted that in this case the correction factor $P$ introduced in Eq. (7) is crucial since a significant part of the 588 $cm^{-1}$ band lies beyond 800 $cm^{-1}$. The correction based on an additional Gaussian band was applied twice, first taking into account only the 588 $cm^{-1}$ band, and then taking into account both the 588 and 140 $cm^{-1}$ bands. It can be seen that the linear correction using Eq. (9) is very close to the linear extrapolation done with the KK procedure. Also, straightforward correction using Eq. (7) with one and two Gaussian terms improve the prediction relative to the linear correction. The relative error at 900 $cm^{-1}$ is 7% with the linear correction, 3.5% with one Gaussian term and 2.6% with the two Gaussians. The correction of the Gaussian addition and the full KKT procedure gives better predictions, although still

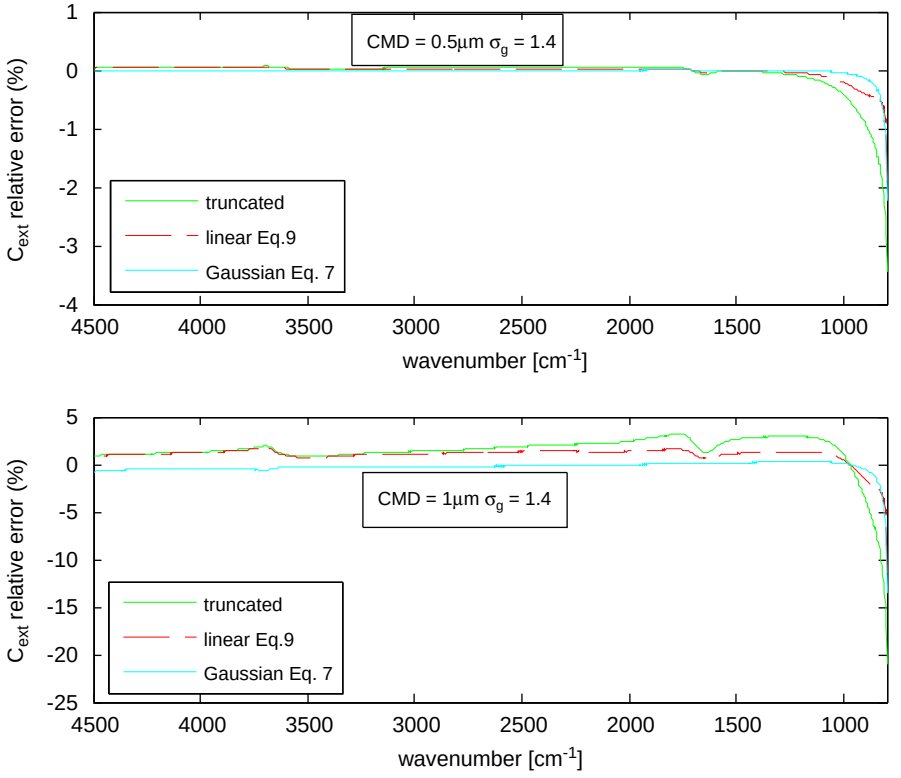


**Fig. 14.** Relative extinction error between "real" extinction cross section calculated with original $k$ and $n$ (the full Bertie and Lan [9] data set), truncated $k$ and $n$, $n$ calculated by Eq. (9), and $n$, calculated by Eq. (7). The calculations were made for spherical water droplets (using the Mie theory) with two different log-normal particle size distributions: (top panel) count median diameter (CMD) of 0.5 μm and a geometric standard deviation ($\sigma_g$) of 1.4, and (bottom panel) CMD of 1 μm and a $\sigma_g$ of 1.4.

not perfect. The main reason for this difference is that Eq. (6) was derived for Gaussian functions with a standard deviation up to 26 $cm^{-1}$, whereas in the water case it is 200. For such a broad band, the assumption that $\sigma$ does not affect $\Delta n$ is obviously not valid anymore. Still, the differences between the predictions of the full KKT procedure and the straightforward corrections using Eq. (7) are relatively small, which demonstrates the validity of the straightforward procedure developed in this work.

Fig. 14 shows how the error in $n$ affects the calculated extinction cross section. The trend is similar to that observed for the ammonium sulfate in Fig. 11: the influence of the error in $n$ on the extinction cross section is relatively low, and is larger for larger particles. In both cases, the optical constants calculated by the method suggested here (Eq. (7)) give a good approximation for the extinction spectrum.

## 4. Conclusions

In any study of optical constants that relies on the KKT to extract the real refractive index $n$ from a measured $k$ spectrum, the integration is either restricted to the measured range of $k$ or to some assumptions regarding the unmeasured spectral range. Hence, it is clear that the results of such studies are influenced by the imaginary refractive index $k$ beyond the range of its actual measurement. Although this influence is well known and documented, it was only reported for specific substances and cases, and the impact of these neglected bands had not been investigated in a systematic fashion. The main objective of this study was to investigate the influence of such unmeasured bands on the extracted $n$ in a systematic manner and to develop simple tools for estimating the resulting errors. This analysis yielded straightforward and relatively simple relationships that can be used to estimate the error in the real refractive index $n(\nu)$ extracted using the Kramers–Kronig transformation procedure when using a truncated $k$ spectrum or a linearly extrapolated spectrum. Additional relationships that describe the contribution of an unmeasured Gaussian or Lorentzian band in the 90–710 $cm^{-1}$ range were also obtained. These relationships can be used for the evaluation of the error size and to correct estimated $n$ values without having to perform the full Kramers–Kronig procedure using an extrapolated $k$ spectrum. These relations were obtained after neglecting the influence of the band shape ($\sigma$). While it was shown that the influence of the band shape is indeed negligible as long as $\sigma \leqslant 26\ cm^{-1}$, one must be aware that applying the same relations for higher values of $\sigma$ may result in lower accuracy (see second case study above). Finally, a relationship that describes the uncertainty (or error) in $n(\nu)$ that result from approximating an unmeasured band using a literature-based band that is not located accurately has also been obtained. These results also showed that mismatch between the shapes of a true (unknown) and literature-based bands causes virtually no error in the estimate of $n(\nu)$.

All the corrective relationships were derived for normalized bands of unit area. Therefore, their use requires not only knowledge about the location of the unmeasured band but also knowledge about its amplitude. In practice this amplitude is never known exactly and the inaccuracy in its estimate will act as a multiplicative factor on the estimated error. Although the requirement that the band amplitude is known is most probably the main obstacle to the use of the proposed method, such information would be required for any correction of the $n$ spectrum obtained by the KKT procedure. The major advantage of the corrective relationships developed in this work is that they allow correction of the $n$ spectrum in a straightforward fashion, without having to recalculate the KK integral.

## Acknowledgment

M. Segal-Rosenheimer would like to thank the Israeli Ministry of Science for its financial support through the Levi Eshkol scholarship.

## References

[1] Bohren CF, Huffman DR. Absorption and scattering of light by small particles. Weinheim: Wiley-VCH; 2004.
[2] Biermann UM, Luo BP, Peter T. Absorption spectra and optical constants of binary and ternary solutions of $H_2SO_4$, $HNO_3$, and $H_2O$ in the mid infrared at atmospheric temperatures. J Phys Chem A 2000;104:783–93.
[3] Boer GJ, Sokolik IN, Martin ST. Infrared optical constants of aqueous sulfate-nitrate-ammonium multi-component tropospheric aerosols from attenuated total reflectance measurements—part I: results and analysis of spectral absorbing features. J Quant Spectrosc Radiat Transfer 2007;108:17–38.
[4] Clapp ML, Miller RE, Worsnop DR. Frequency-dependent optical constants of water ice obtained directly from aerosol extinction spectra. J Phys Chem 1995;99:6317–26.
[5] Dohm MT, Potscavage AM, Niedziela RF. Infrared optical constants of Carvone from the Mie inversion of aerosol extinction spectra. J Phys Chem A 2004;108:5365–76.
[6] Earle ME, Pancescu RG, Cosic B, Zasetsky AY, Sloan JJ. Temperature-dependent complex indices of refraction for crystalline $(NH_4)_2SO_4$. J Phys Chem A 2006;110:13022–8.
[7] Wagner R, Mangold A, Möhler O, Saathoff H, Schnaiter M, Schurath U. A quantitative test of infrared optical constants for supercooled sulphuric and nitric acid droplet aerosols. Atmos Chem Phys 2003;3:1147–64.
[8] Wagner R, Stefan B, Ottmar M, Harald S, Martin S, Schurath U. Mid-infrared extinction spectra and optical constants of supercooled water droplets. J Phys Chem A 2005;109:7099–112.
[9] Bertie JE, Lan Z. Infrared intensities of liquids XX: the intensity of the OH stretching band of liquid water revisited, and the best current values of the optical constants of $H_2O$(l) at 25 °C between 15,000 and 1 $cm^{-1}$. Appl Spectrosc 1996;50:1047–57.

[10] Myhre CEL, Christensen DH, Nicolaisen FM, Nielsen CJ. Spectroscopic study of aqueous $H_2SO_4$ at different temperatures and compositions: variations in dissociation and optical properties. J Phys Chem A 2003;107:1979–91.
[11] Hawranek JP, Neelakantan P, Young RP, Jones RN. Control of errors in Ir spectrophotometry.4. Corrections for dispersion distortion and evaluation of both optical-constants. Spectrochim Acta Part A Mol Biomol Spectrosc 1976;32:85–98.
[12] Steele HM, Eldering A, Lumpe JD. Simulations of the accuracy in retrieving stratospheric aerosol effective radius, composition, and loading from infrared spectral transmission measurements. Appl Opt 2006;45:2014–27.
[13] Bertie JE, Lan Z, Jones N, Apelblat Y. Infrared intensities of liquids XVIII: accurate optical constants and molar absorption coefficients between 6500 and 800 $cm^{-1}$ of dichloromethane at 25 °C, from spectra recorded in several laboratories. Appl Spectrosc 1995;49:840–51.
[14] Niedziela RF, Norman ML, DeForest CL, Miller RE. A temperature- and composition-dependent study of $H_2SO_4$ aerosol optical constants using fourier transform and tunable diode laser infrared spectroscopy. J Phys Chem A 1999;103:8030–40.
[15] Signorell R, Luckhaus D. Aerosol spectroscopy of dihydroxyacetone: gas phase and nanoparticles. J Phys Chem A 2002;106:4855–67.
[16] Segal-Rosenheimer M, Dubowski Y, Linker R. Extraction of optical constants from Mid-IR spectra of small aerosol particles. J Quant Spectrosc Radiat Transfer 2009;110:415–26.
[17] Toon O, Pollack J, Khare B. The optical constants of several atmospheric aerosol species: ammonium sulfate, aluminum oxide, and sodium chloride. J Geophys Res 1976;81:5733.
[18] Niedziela RF, Miller RE, Worsnop DR. Temperature- and frequency-dependent optical constants for nitric acid dihydrate from aerosol spectroscopy. J Phys Chem A 1998;102:6477–84.